Available online at www.sciencedirect.com
ScienceDirect
Journal of the European Ceramic Society 29 (2009) 2061–2068
www.elsevier.com/locate/jeurceramsoc

Advanced coatings on the basis of Si(C)N precursors for protection of steel against oxidation

Martin Günthner [a], Tobias Kraus [a], Andreas Dierdorf [b], Daniel Decker [b], Walter Krenkel [a], Günter Motz [a,*]

[a] *University of Bayreuth, Ceramic Materials Engineering (CME), D-95440 Bayreuth, Germany*
[b] *Clariant Advanced Materials GmbH, D-65843 Sulzbach am Taunus, Germany*

Received 28 August 2008; accepted 11 November 2008
Available online 7 January 2009

Abstract

An effective and low-cost method for applying polysilazane-based barrier coatings on stainless steel is presented. Two different precursors in the system SiCN (ABSE) and SiN (PHPS) have been used for applications of polymeric and ceramic-like coating materials. With corresponding precursor solutions in toluene or ether, steel substrates were coated by means of a simple dip coating technique. The influence of different annealing atmospheres such as ambient air and nitrogen on the resulting coatings was determined. Therefore precursor-based powders and coatings were characterised by TGA, REM, TEM, GDOES and chemical composition measurements. Oxidation tests on coated samples were done in air at temperatures of 800–1000 °C. By measuring the weight gain and the oxidation depth, parabolic oxidation kinetics were determined. The precursor-based coatings protect stainless steel from oxidation up to 1000 °C.

Keywords: Precursor; Surfaces; Oxidation; Si(C)N; Structural applications

1. Introduction

The economic loss caused by wear, oxidation and corrosion of metals is estimated at several milliard € per year. Barrier coatings are widely applied to enhance the behaviour against aggressive environments. Non-oxide and oxide ceramic coatings are promising candidates for improving the resistance against high temperature scaling and oxidation of metals. Mainly deposition methods like thermal spraying,[1] CVD[2] and PVD processes[3] or sol–gel techniques[4,5] are applied for the generation of ceramic coatings. Drawbacks of these well-established techniques are for instance the porosity of the formed coatings (thermal spraying) or the complex and high-priced technologies (e.g. plasma and high vacuum technology). Furthermore, sol–gel coatings are thin and nanoporous.[6]

An alternative, relatively low-cost and easy approach to these methods is the processing of polymeric and ceramic-like coatings by the well-known pyrolysis of appropriate organoelemental compounds (precursors). Coatings are mainly based on silicon containing precursors like polysiloxanes,[7–9] polycarbosilanes[10–12] or polysilazanes.[13–18] The resulting polymer-derived ceramics (PDCs) like silicon oxycarbide (SiCO), silicon carbide (SiC), silicon nitride (Si_3N_4) or silicon carbonitride (SiCN) are promising materials for high temperature applications. They offer excellent properties in thermal shock resistance, creep resistance, high temperature strength and thermal stability.[19–21] The outstanding oxidation behaviour of PDCs has been investigated in several studies.[22–27] The formation and growth of a protective SiO_2 layer, which has the lowest oxygen permeability among all simple oxides, is the main reason for the excellent oxidation resistance of PDCs.[28]

With exception of the polysiloxane systems, most investigations on polymer-derived coatings have been done on coatings pyrolysed in inert atmospheres like argon or nitrogen. Only a few authors describe the treatment of precursor-based coatings in oxygen containing atmospheres like air or helium/oxygen mixtures. A clear incorporation of oxygen into the surface up to a complete transformation into SiO_2 films can be detected.[11,13,16,18]

* Corresponding author. Fax: +49 921 555502.
E-mail address: guenter.motz@uni-bayreuth.de (G. Motz).

0955-2219/$ – see front matter © 2008 Elsevier Ltd. All rights reserved.
doi:10.1016/j.jeurceramsoc.2008.11.013

In this work, we report on the influence of different coating and annealing parameters – especially the handling and pyrolysis atmosphere – on the film formation, the adhesion and the resulting composition of the coatings. A possible treatment in air could simplify the process, since the need of inert atmosphere is often a critical factor for applications of precursor systems. The investigated films are based on the tailored solid and soluble ammonolysed bis(dichlormethyl)silylethane (ABSE) and on perhydropolysilazane (PHPS).

Furthermore, the oxidation protection effect of coated stainless steel substrates was evaluated by weight gain measurements and depth profiles of the chemical composition (diffusion of oxygen). From the achieved data, oxidation kinetics were determined.

2. Experimental procedure

The ABSE polycarbosilazane is synthesised by ammonolysis of bis(dichloromethyl)silyl-ethane in toluene as described elsewhere for other silazanes.[29,30] The synthesis yield of the colourless, brittle and meltable solid is about 75 wt.%. For the coating process, solutions in toluene and ether with low viscosity were used.

The commercially available PHPS polysilazane is produced by ammonolysis of the dichlorosilane SiH_2Cl_2.[31] A solution of maximum 20% by weight in dibutyl ether was used (PHPS NN 120-20, Clariant Advanced Materials GmbH, Sulzbach, Germany).

Flat stainless steel plates (1.4016, 1.4301, thickness 1 mm) were cut into sheets with a size of 2.5 cm × 8 cm, cleaned in acetone by ultrasonic treatment and dried. The samples were dip-coated with a hoisting apparatus and the coating thickness was adjusted by concentrating the solution and by varying the hoisting speed between 0.1 and 0.5 m/min. Annealing of the coated sheets was performed either in air (Nabertherm® LH 60/14, Nabertherm, Lilienthal, Germany) or in nitrogen (O_2 < 50 vpm/F-A 100-500/13, GERO GmbH, Neuhausen, Germany) at 800 °C for 1 h with heating and cooling rates were 3 K/min.

Static, isothermal oxidation tests in air (Nabertherm® LH 60/14) at temperatures between 800 and 1000 °C and holding times from 1 to 100 h were applied.

The coatings were examined by light microscopy, scanning electron microscopy (1540EsB Cross Beam, Carl Zeiss AG, Germany) and transmission electron microscopy (Libra 200 FE, Carl Zeiss AG, Germany). The layer thickness was measured with a Fischerscope® MMS (Helmut Fischer GmbH & Co.KG, Germany) by the eddy current method (ASTM B244) or by the profile method (DIN EN ISO 4287/MFW-250 Mahr GmbH, Germany). The oxidation behaviour and kinetics of the coated and uncoated samples were analysed by determining the weight change, scanning electron microscopy and glow discharge optical emission spectroscopy (GDOES/Spectruma GDA 750, Spectruma Analytik GmbH, Germany).

Furthermore, precursor powder was milled and sieved to a grain size smaller than 32 μm. The powder was pyrolysed either in nitrogen or in air according to the thermal treatment of the coatings and analysed by TGA (Linseis L81 A1550, Linseis, Germany), coupled FTIR (Bruker Vector 22, Bruker Optik GmbH, Germany), coupled MS (ThermoStar GSD 301 T3, Pfeiffer Vacuum GmbH, Germany) and chemical composition measurements (Mikroanalytisches Labor Pascher, Germany).

3. Results and discussion

3.1. Precursor properties and pyrolysis behaviour

The ABSE precursor structure is composed of two structural elements, namely very stable five-membered carbosilazane rings and bridging linear carbosilazane groups (Fig. 1).[32] The melting point is in the range of 90–150 °C depending on the molecular weight.

The PHPS precursor contains no organic groups (Fig. 1). Due to the large amount of Si–H functions, the PHPS is highly reactive especially with hydroxyl groups.[18]

The pyrolysis behaviour of the polysilazanes was characterised by TGA and coupled FTIR and MS measurements to identify gaseous pyrolysis products. Fine precursor powder (<32 μm) was used for the investigations in order to get similar conditions compared to thin films.

As can be seen from Fig. 2, the conversion in nitrogen atmosphere takes place in three steps. The cross-linking of the precursors leading to unmeltable polymers occurs up to 200 °C for PHPS and up to 300 °C for ABSE. No substantial mass loss can be detected in this temperature range.

The intermediate step between 200 and 700 °C (PHPS) or 300 and 800 °C (ABSE) is characterised by a large mass loss because of the transition of the polymers into an amorphous covalent ceramic. Mainly ammonia and methane (ABSE) or SiH species and hydrogen (PHPS) are separated in this temperature range.

Above 700 °C (PHPS) or 800 °C (ABSE), no significant mass changes were observed for both systems. This last pyrolysis step leads to a more compact, structured and rearranged material. The ceramic yield after thermal treatment at 1000 °C is 77 wt.% for ABSE and 85 wt.% for PHPS.

The TGA measurements of the ABSE and PHPS powders in air are given in Fig. 3.

The ABSE precursor shows a similar pyrolysis behaviour in air compared to annealing in nitrogen atmosphere. The main mass loss occurs in the temperature range between 400 and 600 °C by separation of ammonia, methane and hydrogen. The ceramic yield after pyrolysis at 1000 °C increases to a value of 84 wt.%.

For the PHPS system, a remarkable weight gain due to oxidation of free silicon and substitution of nitrogen by oxygen can be detected. The main increase by incorporation of oxygen lies in the temperature range between 150 and 400 °C despite the separation of ammonia and hydrogen in this range. The ceramic yield after pyrolysis at 1000 °C is 118 wt.%. For a complete oxidation into SiO_2, the ceramic yield would be in the range of 143 wt.%.

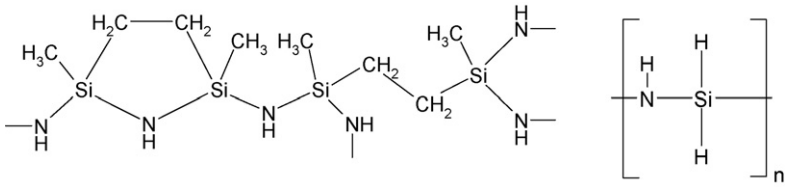

Fig. 1. Basic structure units of the ABSE (left) and PHPS (right) precursor.

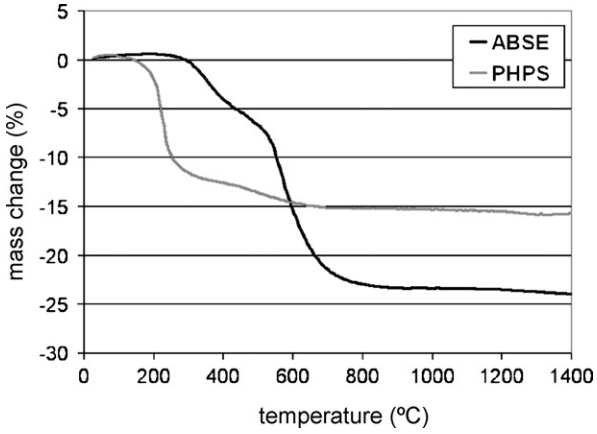

Fig. 2. TG analyses of ABSE and PHPS powders (<32 μm) in nitrogen atmosphere.

Table 1
Chemical composition of the precursors and the resulting ceramic residues.

Polysilazane	Treatment	Empirical formula
ABSE	Initial state	$SiNC_2H_6$
ABSE	1000 °C, 1 h, nitrogen	$SiN_{0.9}C_{1.5}O_{0.2}$
ABSE	1000 °C, 1 h, air	$SiN_{0.02}C_{0.05}O_{1.89}$
PHPS	Initial state	$SiN_{0.81}H_{2.5}$
PHPS	1000 °C, 1 h, nitrogen	$SiN_{0.98}O_{0.03}$
PHPS	1000 °C, 1 h, air	$SiN_{0.47}O_{1.08}$

The chemical composition of the polymers in the initial state and of the ceramic residues after pyrolysis at 1000 °C in nitrogen or air is shown in Table 1.

The chemical analyses indicate that after pyrolysis at 1000 °C in nitrogen the ABSE-based ceramic contains a free carbon content of 32 mol%, whereas the PHPS-based material has an excess of 13 mol% silicon. Schwab et al.[33] and Iwamoto et al.[34] published similar results on PHPS-derived ceramics.

After pyrolysis for 1 h in air the composition of the fine ABSE powder is nearly SiO_2. Bahloul et al.[35] also published the total oxidation of a polycarbosilazane by heat treatment in an oxygen helium mixture at temperatures higher than 500 °C.

For the fine PHPS powder, however, no complete conversion of the polysilazane into SiO_2 under the chosen pyrolysis conditions in air takes place. The residual nitrogen content is in the range of 12 wt.%.

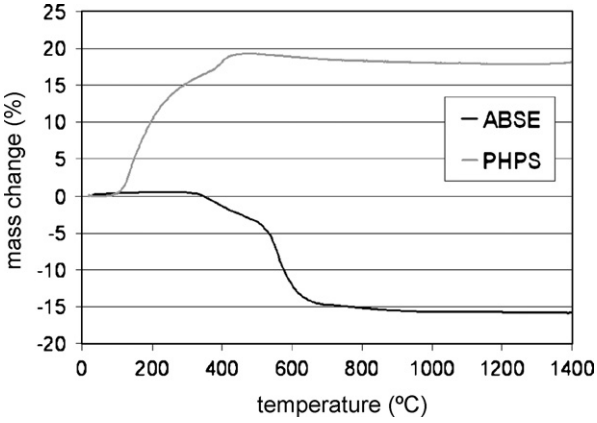

Fig. 3. TG analyses of ABSE and PHPS powders (<32 μm) in air.

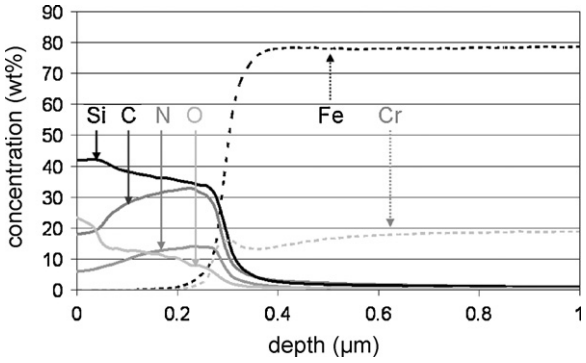

Fig. 4. GDOES concentration–depth profile of an ABSE-based coating on a 1.4016 steel sample after annealing at 800 °C for 1 h in nitrogen.

3.2. Chemical composition of the coatings

The chemical composition of ABSE and PHPS-derived coatings on steel after annealing at 800 °C either in nitrogen or in air is shown in Figs. 4–7 by GDOES depth profiles. Since no significant mass change takes place between 800 and 1000 °C (see Figs. 2 and 3), the elemental compositions of the coatings

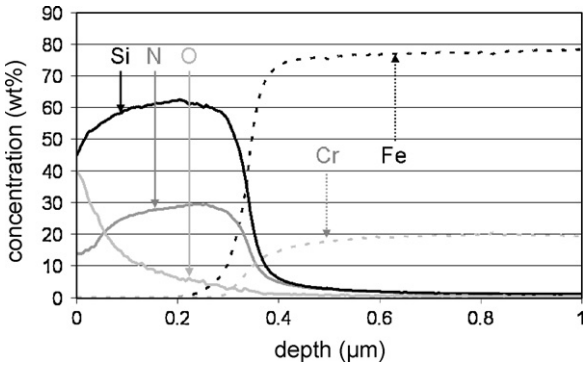

Fig. 5. GDOES concentration–depth profile of a PHPS-based coating on a 1.4016 steel sample after annealing at 800 °C for 1 h in nitrogen.

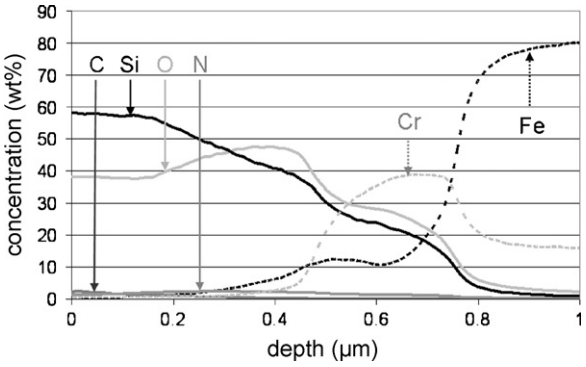

Fig. 6. GDOES concentration–depth profile of an ABSE-derived coating on a 1.4016 steel sample after annealing at 800 °C for 1 h in air.

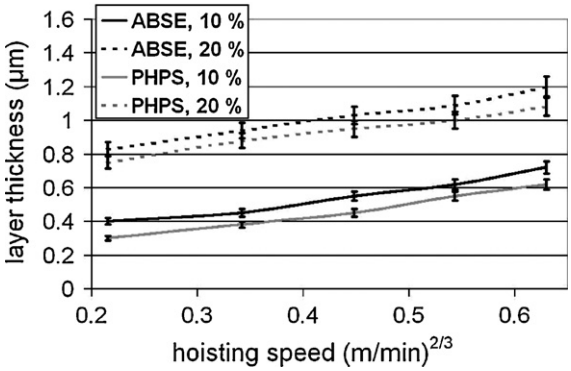

Fig. 8. Thickness of precursor-based coatings on 1.4301 steel samples, treated in air at 500 °C for 1 h.

pyrolysed at 800 °C can be compared to those of the powders treated at 1000 °C (Table 1).

After thermal treatment in nitrogen (Figs. 4 and 5), the coatings consist mainly of Si and N (PHPS) or Si, C, and N (ABSE). Compared to the chemical composition of the precursor powders, a greater incorporation of oxygen into the coatings especially near the surface can be detected, which decreases with coating thickness. The oxygen content originates from the handling and processing of the coatings, where a short exposure to oxygen and moisture could not be avoided, and from the nitrogen atmosphere used for the pyrolysis step, which includes oxygen impurities ($O_2 < 50$ vpm). These results coincide well with the investigations of Colombo and Mucalo.[11–13] They describe a strong dependency of the oxygen purity of the annealing atmosphere on the oxygen content in the coatings.

Figs. 6 and 7 show the ABSE- and PHPS-based coatings after thermal treatment at 800 °C for 1 h in air. A clear incorporation of oxygen into the coatings leading to SiO_x or SiO(N) ceramics can be detected. Whereas the C and N content in the ABSE-based coating is negligibly small, the N content in the PHPS-based film lies between 5 and 10 wt.%.

As can be seen, the results of the GDOES profiles coincide well with the chemical composition measurements on the fine precursor-based powders. After pyrolysis in air at temperatures higher than 800 °C, the composition of the ABSE-derived fine powder and coating is approximately SiO_2. For the PHPS-based material, however, no complete conversion into SiO_2 under the chosen conditions in air takes place. From the measurements, we conclude that the pyrolysis of the PHPS system in air leads to the formation of a compact and dense protective oxide layer at the surface, and therefore to a closed system which retards a total oxidation of the polysilazane material. This protection effect cannot be detected that clearly for the ABSE system.

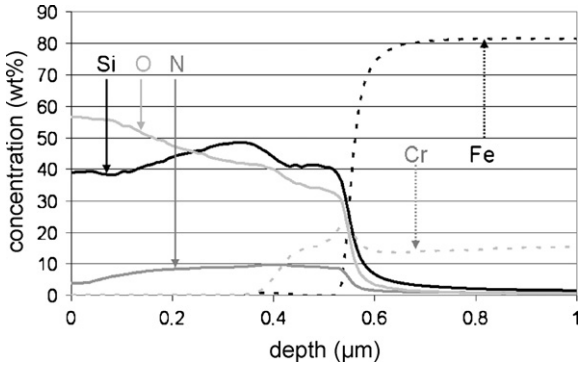

Fig. 7. GDOES concentration–depth profile of a PHPS-derived coating on a 1.4016 steel sample after annealing at 800 °C for 1 h in air.

3.3. Thickness and adhesion of the coatings

Precursor-based coatings on stainless steel substrates were applied from solutions of the precursors in toluene and ether. The layer thickness can be adjusted by the dip coating parameters, especially the concentration or viscosity of the solution and the hoisting speed.[36] Fig. 8 shows the resulting thickness of the silazane-based coatings on polished steel sheets after annealing in air for 1 h at 500 °C as a function of precursor concentration and hoisting speed.

The coating thickness increases with hoisting speed and precursor concentration and attains values between 0.3 and 1.2 µm. SEM investigations show that the precursor-based coatings are dense, uniform and homogeneous. Singular coated films thicker than about 1.5 µm start to crack and split off if the heating rate or pyrolysis temperature is too high. The low viscosity coating solutions wet the substrate very well. Therefore, the roughness of metal surfaces is levelled as presented in Fig. 9.

On steel, a natural oxide layer with adsorbed water is present in air.[37] Polysilazanes react with hydroxyl groups by the following simplified reactions[35]:

$$\text{Fe–OH} + \equiv \text{Si–NH–Si} \equiv \rightarrow \equiv \text{Fe–O–Si} \equiv + \text{H}_2\text{N–Si} \equiv \quad (1)$$

$$\text{Fe–OH} + \text{H}_2\text{N–Si} \equiv \rightarrow \equiv \text{Fe–O–Si} \equiv + \text{NH}_3 \quad (2)$$

We conclude that direct chemical metal–O–Si bonds between the steel and the precursor-based coatings are formed. Thus, the adhesion of the precursor layers on metals should be very good.

The adhesion pull-off strength of the coatings (ASTM D 4541) with a value higher than 38 N/mm^2 supports our conclusion.

Furthermore, the excellent adhesion of the films via chemical bonding leads to the interdiffusion of the coating and the base material after pyrolysis in air at 800 °C. Chromium from the stainless steel diffuses into the coating, forming a diffusion layer

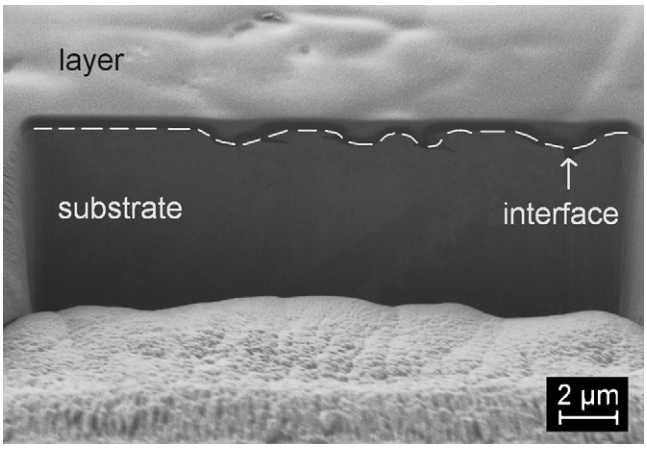

Fig. 9. Scanning electron micrograph of a PHPS-coating on stainless steel 1.4301, treated at 500 °C for 1 h in air; cross-section prepared with the Focused Ion Beam (FIB) technique.

with a composition of Si, O and Cr at the interface (Figs. 6 and 7). This fact is also shown by a TEM micrograph in Fig. 10, where the diffusion layer can be clearly seen in the cross-section as a brighter region at the interface.

3.4. Oxidation protection of steel

To investigate the protection effect of precursor-based coatings on stainless steel, different parameters – especially the layer thickness, the annealing temperature, the annealing atmosphere and the precursor system – were varied. The main question was how the different polymer architecture, composition and pyrolysis behaviour of the two precursors ABSE and PHPS influence the oxidation protection effect on steel.

As can be seen from Figs. 6 and 7, the handling and annealing of the precursor coatings on stainless steel in air lead to a strong incorporation of oxygen into the layers. Therefore, the mass loss and the shrinkage due to the conversation of the polymer into a ceramic are smaller in comparison to the pyrolysis in nitrogen

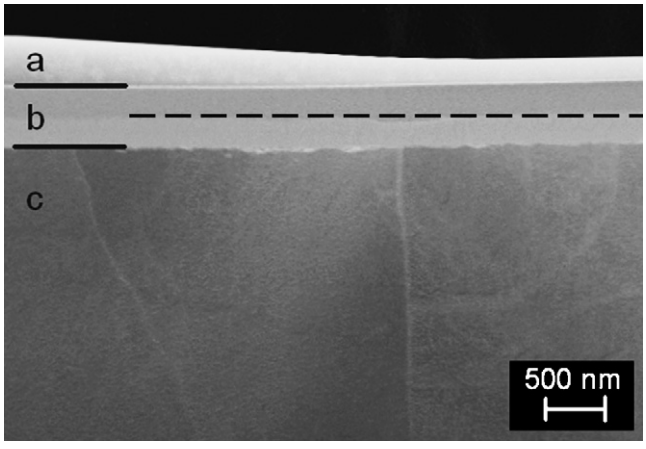

Fig. 10. TEM dark field micrograph of a PHPS-derived coating on 1.4016 steel in cross-section, pyrolysed at 800 °C for 1 h in air (a: tungsten protective layer for preparation, b: ceramic-like coating with diffusion layer (brighter region), c: steel sheet).

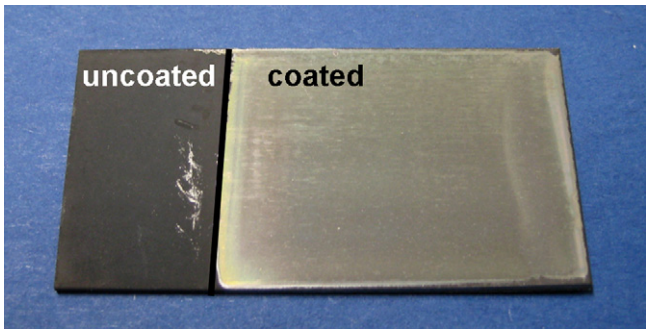

Fig. 11. Digital image of a 1.4301 steel sheet dip-coated with PHPS, oxidised at 1000 °C for 1 h in air.

(see Figs. 2 and 3). This enables thicker coatings without cracks and therefore a better protection effect against oxidation could be observed. Because of this, only the results of the optimised ceramic coatings which were initially pyrolysed in air at 800 °C for 1 h are presented in the following discussion.

Static isothermal oxidation tests were performed in air at temperatures between 800 and 1000 °C for 1–100 h.

As shown in Fig. 11, a dark oxide film is formed on uncoated stainless steel regions, whereas the precursor-coated area shows the original metallic gloss up to an oxidation temperature of 1000 °C.

SEM micrographs of coated and oxidised sheets are presented in Figs. 12 and 13. Fig. 12 shows an oxidised sample at the transition of a PHPS-coated (above) to the uncoated region (below). Whereas crystalline chromium oxides can be seen on uncoated areas, the precursor coating passivates the substrate very well.

This fact is also shown in Fig. 13, where the growing of chromium oxides through a crack of the PHPS-coating after oxidation at 1000 °C can be seen. Cracks only appear at the edges or near the border areas of the steel samples due to dip coating inhomogeneities. Altogether, the SEM studies show that the precursor layers are dense, protective, free of bubbles and almost free of cracks, whereas uncoated stainless steel oxidises at temperatures higher than 800 °C by the formation of mainly chromium oxides.

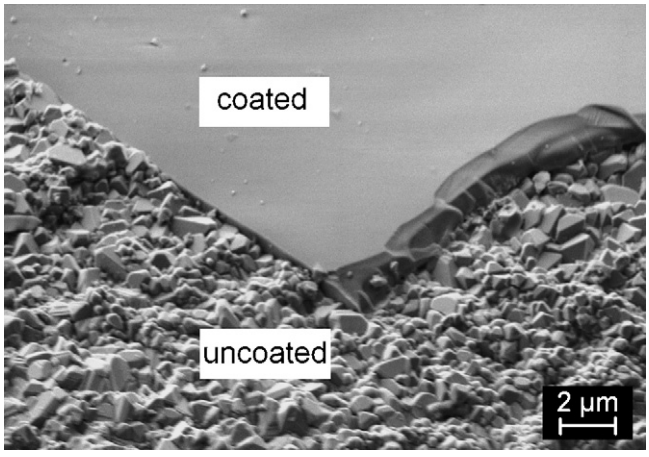

Fig. 12. SEM micrograph of an oxidised (1000 °C, 1 h, air) 1.4301 steel sample at the transition of PHPS-coated (above) and uncoated (below) region.

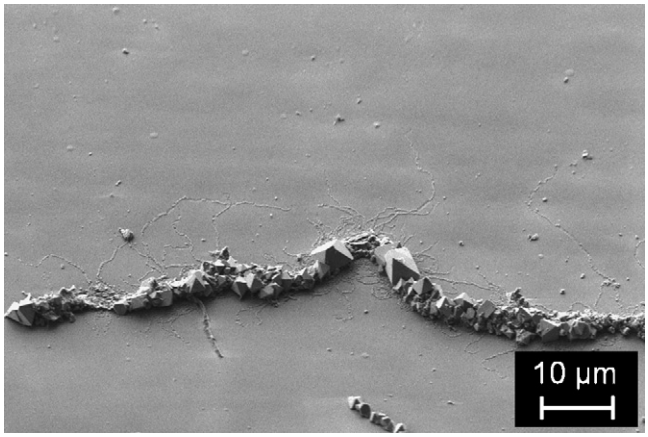

Fig. 13. SEM micrograph of a PHPS-coated and at 1000 °C for 1 h oxidised 1.4301 steel sample.

For the evaluation of the oxidation kinetic mechanism, the weight gain or the oxide scale thickness as a function of oxidation time must be determined. Both values were measured. By plotting the weight gain as a function of oxidation time, a parabolic oxidation kinetic law could be observed. This is due to the oxidation mechanism of silica former, where the oxygen diffusion through a growing dense and protective oxide layer is the rate-limiting process.[28] But for investigating and comparing oxidation kinetics, the measurement of the oxide film thickness is more meaningful than the determination of the weight gain, since the oxidation of different material systems leads to different mass changes.[22] Therefore, depth profile measurements were conducted by GDOES.

Fig. 14 shows the oxygen depth profiles of uncoated, ABSE and PHPS-coated steel samples, which were initially annealed in air at 800 °C for 1 h and then oxidised at 1000 °C for 10 h. As can be seen from the figure, oxygen diffuses into the uncoated stainless steel sheet to a depth of about 7 µm, whereas the oxidation depth of both precursor-coated samples is much smaller. Due to the rapid decrease of the oxygen concentration, the PHPS-coating acts as the most effective diffusion barrier.

For the calculation of kinetic data, the oxide layer thickness must be determined. Because of the lack of a standard method for calculating the silica thickness from GDOES profiles, the oxide

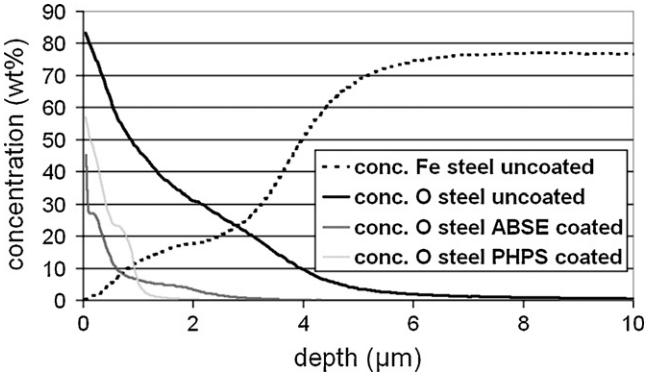

Fig. 14. GDOES concentration–depth profiles of different 1.4301 steel samples (uncoated, ABSE or PHPS-coated and initially pyrolysed at 800 °C for 1 h in air) after oxidation at 1000 °C for 10 h.

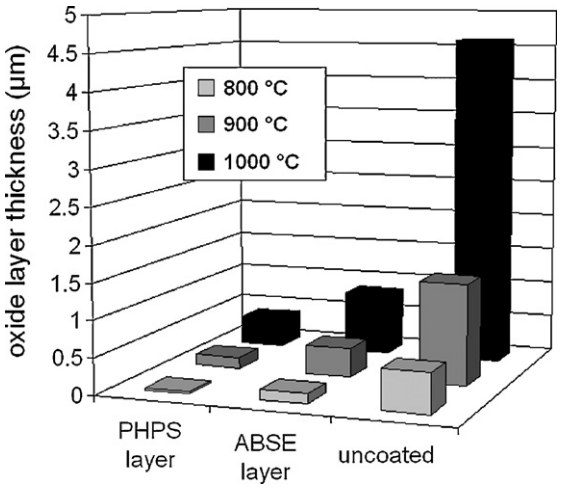

Fig. 15. Oxide layer thickness of uncoated and PHPS or ABSE-coated (initially pyrolysed at 800 °C for 1 h in air) 1.4301 steel samples after oxidation in air for 10 h and temperatures up to 1000 °C, calculated from GDOES measurements.

layer thickness was taken as the depth value, at which the oxygen content is reduced to 5% by weight in the GDOES profiles. Analyses of LM and SEM cross-section micrographs support the thickness values based on the GDOES measurements. Beyond the precursor-coated samples, which were pyrolysed at 800 °C for 1 h in air, a starting oxide layer thickness of 600 nm is considered (see Figs. 6 and 7). The oxide layer thicknesses of precursor-coated and pyrolysed or uncoated 1.4301 steel samples after oxidation in air at different temperatures are shown in Fig. 15.

The parabolic kinetic constant can be calculated from the oxide layer thickness $x(t)$ by the following equation:

$$X^2(t) - X_0^2 = K_T \times t \tag{3}$$

where K_T is the kinetic constant at the temperature T, t is the time and x_0 is the thickness of the silica layer for $t = 0$.

K_T follows the Arrhenius law (4):

$$\ln K_T = \ln K_0 - \frac{E_a}{RT} \tag{4}$$

where K_0 is a pre-exponential parameter, R the ideal gas constant and E_a the apparent activation energy.[23]

The thermal dependence of the oxidation kinetic constant K_T of different samples is presented in an Arrhenius plot in Fig. 16.

Fig. 16 shows that the parabolic oxidation kinetic constants of precursor-coated and in air pyrolysed sheets are as far as to two orders in magnitude smaller than that of the stainless steel 1.4301. Especially the increase of the oxidation constant of uncoated stainless steel at 1000 °C can be effectively reduced by the coatings.

As can be seen from the oxidation studies, the best results are achieved with SiO(N)-gradient coatings about 1 µm in thickness. The shrinkage of the precursor coating during annealing and the thermal expansion of the steel cause cracks if the coatings are too thick. Annealing at a temperature of 800 °C for 1 h is sufficient to generate ceramic-like coatings. Furthermore, the TGA investigations (see Figs. 2 and 3) showed that the weight

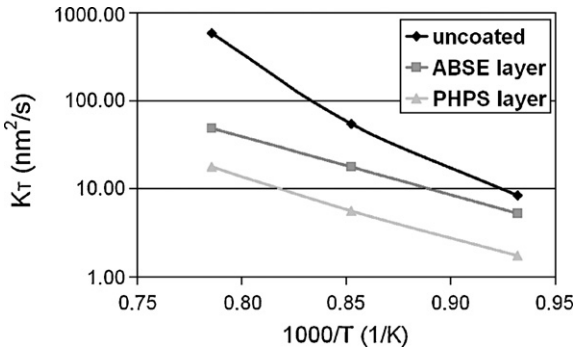

Fig. 16. Arrhenius plot showing the thermal dependence of the oxidation parabolic kinetic constant (K_T) in air for uncoated and ABSE or PHPS-coated (initially pyrolysed at 800 °C for 1 h in air) 1.4301 steel samples.

gain/loss of the precursors between 800 and 1000 °C is negligibly small so that the mass changes can be clearly attributed to the oxidation of the steel samples.

The precursor-based coatings act as an effective diffusion barrier forming a complex, amorphous and gradient Si(N)CrO layer at the surface after thermal treatment in air. The same parabolic oxidation mechanism that was published by Chollon[23] for ceramic fibres can be found for precursor coatings on steel.

PHPS films show a better protection effect than ABSE-based coatings. This is due to the higher ceramic yield of the PHPS system, resulting in very dense, well adherent and passivating barrier coatings. Furthermore, the free Si content in the PHPS precursor system offers a self-healing effect because of the formation of additional SiO_2 at high temperatures (Eq. (5)):

$$Si_{free} + O_2 \rightarrow SiO_2 \quad \text{(PHPS)} \tag{5}$$

The oxidation category temperature of 800 °C for the examined steel grades, which represents the maximal temperature for using in air,[38] can be improved up to 1000 °C by the coatings. This means, that for high temperature applications without very high tribological stresses, special steel grades or refractory alloys could be replaced, leading to reduced costs and partially simpler processing properties.

4. Conclusion

The special tailored ABSE precursor and the commercially available PHPS polysilazane are very suitable to protect metals from oxidation. The coatings can be applied by simple dip- and spray-coating techniques. Due to the reactivity of the silazanes, direct chemical bonds between the coating and the substrate are formed, leading to excellent adhesion.

After thermal treatment at temperatures higher than 800 °C, ceramic-like gradient coatings on stainless steel are generated. The resulting composition of the coatings mainly depends on the pyrolysis atmosphere. Precursor-based coatings protect stainless steel sheets (e.g. AISI 304) from oxidation up to 1000 °C. The resulting gradient Si(N)CrO-layers in the surface act as an excellent diffusion barrier against oxygen and reduce the weight gain and the oxidation kinetic constant up to two orders in magnitude.

Acknowledgments

The Stiftung Industrieforschung, Cologne, Germany and the DFG (Deutsche Forschungsgemeinschaft), Bonn, Germany are acknowledged for financial support. The authors thank the chair of metallic materials at the University of Bayreuth for the support in GDOES, REM and TEM measurements.

References

1. Limarga, A. M., Widjaja, S. and Yip, T. H., Mechanical properties and oxidation resistance of plasma-sprayed multilayered Al_2O_3/ZrO_2 thermal barrier coatings. *Surf. Coat. Technol.*, 2005, **197**, 93–102.
2. Probst, D., Hoche, H., Zhou, Y., Hauser, R., Stelzner, T., Scheerer, H. *et al.*, Development of PE-CVD Si/C/N:H films for tribological and corrosive complex-load conditions. *Surf. Coat. Technol.*, 2005, **200**, 355–359.
3. Allebrandt, D., Hoche, H., Scheerer, H., Broszeit, E. and Berger, C., Oxidation resistance of SiAlCN: H-coatings. *Surf. Coat. Technol.*, 2007, **201**, 5172–5175.
4. Izumi, K., Minami, N. and Uchida, Y., Sol–gel derived coatings on steel sheets. *Key Eng. Mater.*, 1998, **150**, 77–88.
5. Sanctis, O., De Gomez, L. and Pellegri, N., Protective glass coatings on metallic substrates. *J. Non-Cryst. Sol.*, 1990, **121**, 338–343.
6. Bach, F.-W., Möhwald, K., Laarmann, A. and Wenz, T., *Moderne Beschichtungsverfahren (Modern Coating Technologies)*. Wiley–VCH, Weinheim, Germany, 2005.
7. Torrey, J. D., Bordia, R. K., Henager Jr., C. H., Blum, Y., Shin, Y. and Samuels, W. D., Composite polymer derived ceramic system for oxidizing environments. *J. Mater. Sci.*, 2006, **41**, 4617–4622.
8. Torrey, J. D. and Bordia, R. K., Processing of polymer-derived ceramic composite coatings on steel. *J. Am. Ceram. Soc.*, 2008, **91**(1), 41–45.
9. Torrey, J. D. and Bordia, R. K., Mechanical properties of polymer-derived ceramic composite coatings on steel. *J. Eur. Ceram. Soc.*, 2008, **28**, 253–257.
10. Colombo, P., Paulson, T. E. and Pantano, C. G., Synthesis of silicon carbide thin films with polycarbosilane (PCS). *J. Am. Ceram. Soc.*, 1997, **80**, 2333–2340.
11. Colombo, P., Paulson, T. E. and Panano, C. G., Atmosphere effects in the processing of silicon carbide and silicon oxycarbide thin films and coatings. *J. Sol–Gel. Sci. Technol.*, 1994, **2**, 601–604.
12. Mucalo, M. R. and Milestone, N. B., Preparation of ceramic coatings from pre-ceramic precursors. Part II. SiC on metal substrates. *J. Mater. Sci.*, 1994, **29**, 5934–5946.
13. Mucalo, M. R., Milestone, N. B., Vickridge, I. C. and Swain, M. V., Preparation of ceramic coatings from pre-ceramic precursors. Part I. SiC and "Si_3N_4/Si_2N_2O" coatings on alumina substrates. *J. Mater. Sci.*, 1994, **29**, 4487–4499.
14. Greil, P., Polymer derived engineering ceramics. *Adv. Eng. Mater.*, 2000, **2**, 339–348.
15. Kroke, E., Li, Y.-L., Konetschny, C., Lecomte, E., Fasel, C. and Riedel, R., Silazane derived ceramics and related materials. *Mater. Sci. Eng.*, 2000, **26**, 97–199.
16. Lukacs, A., Polysilazane precursors to advanced ceramics. *Am. Ceram. Soc. Bull.*, 2007, **86**, 9301–9306.
17. Cross, T. J. and Raj, R., Synthesis and tribological behavior of silicon oxycarbonitride thin films derived from poly(urea)methyl vinyl silazane. *Int. J. Appl. Ceram. Technol.*, 2006, **3**(2), 113–126.
18. Bauer, F., Decker, U., Dierdorf, A., Ernst, H., Heller, R., Liebe, H. *et al.*, Preparation of moisture curable polysilazane coatings. Part I. Elucidation of low temperature curing kinetics by FT-IR spectroscopy. *Prog. Org. Coat.*, 2005, **53**, 183–190.
19. Riedel, R., Mera, G., Hauser, R. and Klonczynski, A., Silicon-based polymer-derived ceramics: synthesis properties and applications—a review. *J. Ceram. Soc. Jpn.*, 2006, **114**(6), 425–444.
20. Seifert, H. J., Peng, J., Lukas, H. L. and Aldinger, F., Phase equilibria and thermal analysis of Si–C–N ceramics. *J. Alloys Compd.*, 2001, **320**, 251–261.

21. Kollenberg, W., *Technische Keramik (Technical Ceramics)*. Vulkan-Verlag, Essen, Germany, 2004.
22. Nickel, K. G., Corrosion: no problem for precursor-derived covalent ceramics? In *Precursor Derived Ceramics*, ed. J. Bill, F. Wakai and F. Aldinger. Wiley–VCH, Weinheim, Germany, 1999, pp. 188–196.
23. Chollon, G., Oxidation behavior of ceramic fibres from the Si–C–N–O system and related sub-systems. *J. Eur. Ceram. Soc.*, 2000, **20**, 1959–1974.
24. Jacobson, N. S., Opila, E. J. and Lee, K. N., Oxidation and corrosion of ceramics and ceramic matrix composites. *Curr. Opin. Solid State Mater. Sci.*, 2001, **5**, 301–309.
25. Raj, R., An, L. and Shah, S., Oxidation kinetics of an amorphous silicon carbonitride ceramic. *J. Am. Ceram. Soc.*, 2001, **84**, 1803–1810.
26. Ziegler, G., Kleebe, H. J., Motz, G., Müller, H., Traßl, S. and Weibelzahl, W., Synthesis, microstructure and properties of SiCN ceramics prepared from tailored polymers. *Mater. Chem. Phys.*, 1999, **61**, 55–63.
27. Brand, S., Dierdorf, A., Liebe, H., Osterod, F., Motz, G. and Günthner, M., Polysilazane enthaltende Beschichtungen zur Vermeidung von Zunderbildung und Korrosion (Polysilazane based coatings for protection against oxidation and corrosion). DE patent, DE 10 2006 008 308 A1, 2007.
28. An, L., Wang, Y., Bharadwaj, L., Zhang, L., Fan, Y. *et al.*, Silicoaluminium carbonitride with anomalously high resistance to oxidation and hot corrosion. *Adv. Eng. Mater.*, 2004, **6**, 337–340.
29. Motz, G., Hacker, J. and Ziegler, G., Special modified silazanes for coatings, fibers and CMCs. *Ceram. Eng. Sci. Proc.*, 2000, **21**, 307–314.
30. Traßl, S., Suttor, D., Motz, G., Rößler, E. and Ziegler, G., Structural characterization of silicon carbonitride ceramics derived from polymeric precursors. *J. Eur. Ceram. Soc.*, 2000, **20**, 215–225.
31. Seyferth, D. and Wiseman, G. H., High-yield synthesis of Si_3N_4/SiC ceramic materials by pyrolysis of a novel polyorganosilazane. *J. Am. Ceram. Soc.*, 1984, **67**, 132.
32. Motz, G. and Ziegler, G., Simple processibility of precursor-derived SiCN coatings by optimized precursors. In *Proceedings of the Seventh Conference and Exhibition of the European Ceramic Society, vol. 1*, 2001, pp. 475–478.
33. Schwab, S. T., Graef, R. C., Blanchard, C. R., Dec, S. F. and Maciel, G. G., The pyrolytic conversation of perhydropolysilazane into silicon nitride. *Ceram. Int.*, 1998, **24**, 411–414.
34. Iwamoto, Y., Völger, W., Kroke, E. and Riedel, R., Crystallization behavior of amorphous silicon carbonitride ceramics derived from organometallic precursors. *J. Am. Ceram. Soc.*, 2001, **84**(101), 2170–2178.
35. Bahloul, D., Pereira, M. and Goursat, P., Preparation of silicon carbonitrides from organosilicon polymer. I. Thermal decomposition of the cross-linked polysilazane. *J. Am. Ceram. Soc.*, 1993, **76**(5), 1156–1162.
36. Brinker, C. J. and Scherer, G. W., *Sol–Gel Science*. Academic Press, Inc., Boston, 1990.
37. Trostmann, K.-H., *Korrosion (Corrosion)*. Wiley–VCH, Weinheim, Germany, 2001.
38. Manufacturer's data, Tyssenkrupp AG, Germany, 2007.